Preprints.org

Article

Not peer-reviewed version

A Defaultable-Commodity Framework for Compute Capacity Contracts

Zeyu Cao * and Shaosai Huang *

Posted Date: 23 June 2026

doi: 10.20944/preprints202606.1651.v1

Keywords: compute capacity contracts; GPU pricing; defaultable claims; commodity finance; non-storable underlying; lifecycle obsolescence

Preprints.org is a free multidisciplinary platform providing preprint service that is dedicated to making early versions of research outputs permanently available and citable. Preprints posted at Preprints.org appear in Web of Science, Crossref, Google Scholar, Scilit, Europe PMC, OpenAlex.

Copyright: This open access article is published under a Creative Commons CC BY 4.0 license, which permit the free download, distribution, and reuse, provided that the author and preprint are cited in any reuse.

Preprints.org (www.preprints.org) | NOT PEER-REVIEWED | Posted: 23 June 2026 doi:10.20944/preprints202606.1651.v1

Disclaimer/Publisher's Note: The statements, opinions, and data contained in all publications are solely those of the individual author(s) and contributor(s) and not of MDPI and/or the editor(s). MDPI and/or the editor(s) disclaim responsibility for any injury to people or property resulting from any ideas, methods, instructions, or products referred to in the content.

Article

A Defaultable-Commodity Framework for Compute Capacity Contracts

Zeyu Cao [1,*] and Shaosai Huang [2,*]

[1] Independent Researcher, Long Island City, NY 11101, USA
[2] Kspectra Research Inc., Toronto, ON, M2N 0G3, Canada
* Correspondence: josephcao891011@gmail.com (Z.C.); arthur.foxie.huang@kspectra.ai (S.H.)

Abstract

Reserved compute capacity is increasingly tradable amid surging AI-infrastructure investment: in large wholesale blocks and, more recently, through exchange-listed and cleared instruments. Yet pricing a compute capacity contract — a defaultable claim on a non-storable good that obsolesces on a known hardware cadence, sold by issuers that may fail in structurally distinct ways — still falls in the gap between standard commodity and credit finance. We develop a single-issuer pricing framework for this emerging asset class, adapting reduced-form credit intensity and Föllmer–Schweizer hedging to its defining features. The framework is closed-form under affine intensity and is exercised on an H100 forward through the H100→B200 transition.

Keywords: compute capacity contracts; GPU pricing; defaultable claims; commodity finance; non-storable underlying; lifecycle obsolescence

JEL Classification: G12; G13; G32

1. Introduction

Tradeable claims on future compute capacity are emerging at institutional scale: multi-billion-dollar wholesale transfers are disclosed (e.g., xAI [1]; Core Scientific, Inc. [2]; Hut 8 Corp. [3]; Applied Digital Corporation [4]; S&P Global Market Intelligence [5]); three regulated venues have launched cleared GPU-rental derivatives within six months (CME Group and Silicon Data [6]; Intercontinental Exchange [7]; Architect Financial Technologies [8]), cash-settled against an index with no issuer to deliver or default; and exchange-listed reservations trade alongside 24/7 DePIN secondary markets and partially-transferable hyperscaler reservations (Compute Exchange [9]; Amazon Web Services [10]). Valuation demand is rising, yet standard models miss two features that leave the market incomplete: multi-modal issuer non-performance and hardware obsolescence are jumps no traded instrument spans, so no unique arbitrage price exists. This paper proposes an issuer-agnostic pricing framework for the compute capacity contract, applied to a single defaultable issuer, its type entering only through calibrated inputs.

We price the compute capacity contract as a defaultable claim on a commodity forward. The market is incomplete, so we price and hedge by local risk-minimization under the minimal martingale measure (Section 6; Föllmer and Sondermann [11]; Föllmer and Schweizer [12]; Biagini and Cretarola [13]; Bielecki et al. [14]), which leaves the unspanned residual unpriced. Hardware obsolescence is the distinctive feature of the compute capacity contract: unlike a conventional commodity, the delivered good loses value as each successor generation ships. Obsolescence follows each manufacturer's roadmap rather than a common schedule, so depreciation is a roadmap-anchored lifecycle process, not a fitted stationary rate. We adopt Cox reduced-form credit-intensity (Lando [15]; Duffie et al. [16]) with intensities affine in the state — the leading-order (linearization) specification that keeps pricing closed-form and calibratable from sparse data — and one discrete lifecycle Markov chain

© 2026 by the author(s). Distributed under a Creative Commons CC BY license.

Preprints.org (www.preprints.org) | NOT PEER-REVIEWED | Posted: 23 June 2026 doi:10.20944/preprints202606.1651.v1

$\zeta(g,t)$ governs a single depreciation that enters both branches: its rate $\eta^g(\zeta)$ is the commodity drift (Section 4), and its accumulated depth the loading $\beta^{\text{lifecycle}} D(\zeta)$ on the bankruptcy intensity ((11)), so obsolescence raises default risk exactly as it erodes value. Here g is the hardware grade vector, taken as an exogenous parameter (Section 2). The credit–value coupling is then structural and roadmap-pinned, fixed *ex ante* from the lifecycle rather than calibrated as a free parameter (cf. Hull and White [17]; Capponi et al. [18]; Frye [19]; Brigo et al. [20]). For a single issuer the level of this loading is set by the issuer's own credit spread, while its variation across lifecycle states follows the roadmap depth ratio; cross-issuer exposure heterogeneity, through architecture-concentration and common-shock-clustering channels (diversified-cloud to grade-concentrated issuers), is the subject of the multi-issuer companion (Cao and Huang [21]). The nearest existing work prices compute as a good (commodity-finance and derivatives pricing, e.g., the inference-token futures of Xing [22]; the cleared index venues above), not a bilateral claim on a defaultable issuer with obsolescence as a joint driver. The framework fills that role, valuing the single-name, deliverable contract that actually transacts: a fair-value and credit-adjustment reference on top of the cleared index.

In this paper, we condition on the observed spot $P^{g,\text{spot}}(t)$; its endogenous dynamics lie outside scope. We likewise exclude the non-transferable limit, in which the tradeability friction diverges (Section 3).

2. The Compute Capacity Contract

The unit of analysis is the **compute capacity contract**: a contractual right entitling the holder to one unit of compute capacity at a specified hardware configuration from a specified issuer during a specified delivery window. The capacity-unit is most commonly one GPU-instance-hour but the framework applies equally to TPU-hours, Trainium-hours, Ascend-hours, and other architecture variants. Settlement may be token-based, database-recorded, or paper-based.

Definition 1 (Compute capacity contract)**.** *A* compute capacity contract *is a tuple* $(i, g, T, \mathcal{S}, V)$ *where* i *is the issuer,* g *is the grade vector specifying the hardware configuration,* T *is the delivery period,* $\mathcal{S}$ *is the settlement mechanism, and* V *is the value of the holder's entitlement. The contract entitles the holder to one unit of compute capacity at grade* g *from issuer* i *during* T*, subject to issuer* i*'s SLA and continuity.*

The grade g is a multi-dimensional vector taken as exogenous, in the standard commodity-finance treatment of grade as an industry-defined attribute (Tvedt [23]; Koekebakker et al. [24]). Table 1 catalogs the dimensions used in this paper; architecture family and generation set the lifecycle state of Section 4.

Table 1. Grade-vector dimensions used in single-issuer pricing.

Dimension	Illustrative values	Pricing relevance
Architecture family	NVIDIA Hopper/Blackwell, Google TPU, AWS Trainium, Huawei Ascend, AMD Instinct	First-order; sets the lifecycle states
Generation / model	H100, H200, B100, B200, B300, TPU v5p, Trainium 2	First-order; within family, fixes the current lifecycle state
Interconnect	Within-node NVLink, cross-node InfiniBand or Ethernet	First-order for multi-node training workloads
Service tier	Bare-metal, managed-service, full-SLA	Often first-order; managed-service trades at 2–3× bare-metal

3. Two-Channel Pricing

A compute capacity contract is structurally a defaultable claim: the payoff depends jointly on issuer continuity (a credit-branch question) and on the value of the delivered capacity-unit at delivery (a commodity-branch question). Pricing therefore needs both machineries layered through a common pricing equation. We fix a single issuer throughout this paper and suppress the issuer subscript i on

© 2026 by the author(s). Distributed under a Creative Commons CC BY license.

Preprints.org (www.preprints.org) | NOT PEER-REVIEWED | Posted: 23 June 2026 doi:10.20944/preprints202606.1651.v1

all symbols, restoring named subscripts only for the cross-sectional comparison of Section 7. Here, $F^g(t,T)$ denotes the time-t forward price for delivery at T of one grade-g capacity-unit from the issuer — a defaultable claim whose delivery is contingent on issuer survival and SLA performance. We model on a filtered probability space $(\Omega, \mathcal{F}, (\mathcal{F}_t)_{t\in[0,T]}, \mathbb{P})$ satisfying the usual conditions, where $\mathbb{P}$ is the physical (real-world) measure — under which the spot, default, and lifecycle dynamics evolve and are calibrated — and $\mathbb{F} = (\mathcal{F}_t)$ is the market filtration to which all processes are adapted. We price under a measure $\tilde{\mathbb{Q}}$ equivalent to $\mathbb{P}$. Compute markets are radically incomplete: the default time τ^{term}, recovery, and operational loss are not spanned by the tradeable spot $P^{g,\text{spot}}$, so no self-financing spot position replicates the claim and the equivalent martingale measure is not unique. We take $\tilde{\mathbb{Q}}$ to be the minimal martingale measure (MMM) of Föllmer and Schweizer [12], extended to defaultable claims by Biagini and Cretarola [13]: it prices the spanned commodity risk by no-arbitrage and assigns *zero* risk premium to the orthogonal, unhedgeable residual (default timing, recovery, operational loss), which the Föllmer–Schweizer local-risk-minimizing decomposition — the hedging counterpart of the MMM, developed in Section 6 — isolates as L^{FS}. This is a convention, not a no-arbitrage consequence: risk-averse pricing (e.g., minimal-entropy or utility-indifference) would load a positive premium on that residual, an out-of-model add-on. The affine specification of Section 6 satisfies the Biagini–Cretarola structure condition under which the MMM is well-defined.

Derivation.

Fix the trade time $t < T$. Let τ^{term} denote the terminal failure stopping time (specified in Section 5), and let $\Pi^g(T)$ denote the realized time-T market value per delivered capacity-unit. The terminal event partitions paths: $\{\tau^{\text{term}} > T\}$ delivers capacity at T; $\{\tau^{\text{term}} \le T\}$ settles via cause-conditional recovery; operational losses accumulate throughout the survival period. We take τ^{term} to be a doubly-stochastic (Cox) default time (Lando [15]; Duffie and Singleton [25]): the first instant an affine intensity λ^{term} crosses an independent unit-exponential threshold. This makes τ^{term} totally inaccessible with an affine hazard (the closed-form survival of Section 6) and satisfies the H-hypothesis (Bielecki and Rutkowski [26]), so the survival indicator and delivered value factorize conditional on the factor path, their unconditional covariance carried by the correction Γ below. Setting

$$
\begin{aligned}
S(t,T) &= \mathbb{E}^{\tilde{\mathbb{Q}}}[\mathbf{1}_{\{\tau^{\text{term}}>T\}} \mid \mathcal{F}_t] && \text{(survival probability)},\\
G^g(t,T) &= \mathbb{E}^{\tilde{\mathbb{Q}}}[B(t,T)\,\Pi^g(T) \mid \mathcal{F}_t] && \text{(survival-conditional forward)},\\
L^{\text{recovery}}(t,T) &= \mathbb{E}^{\tilde{\mathbb{Q}}}\big[\mathbf{1}_{\{\tau^{\text{term}}\le T\}} B(t,\tau^{\text{term}})\,R\,V \mid \mathcal{F}_t\big] && \text{(expected recovery)},\\
L^{\text{op}}(t,T) &= \mathbb{E}^{\tilde{\mathbb{Q}}}\Big[\textstyle\int_t^{T\wedge\tau^{\text{term}}} B(t,s)\,\ell^{\text{op}}(s)\,dN^{\text{op}}(s) \mid \mathcal{F}_t\Big] && \text{(expected operational loss)},
\end{aligned}
$$

the three streams collapse to the pricing equation

$$
F^g(t,T) \;=\; S(t,T)\,G^g(t,T)\,e^{-\Gamma(t,T)} \;+\; L^{\text{recovery}}(t,T) \;-\; L^{\text{op}}(t,T), \tag{1}
$$

where $B(t,T)$ is the risk-free discount factor; in the recovery term $R\,V$, the face value V is fixed (the contract's purchase price, Definition 1) and the recovery rate $R \in [0,1]$ is *cause-conditional* — it equals the rate $R^{(\kappa)}$ of whichever cause κ ends the contract, resolved over causes in Section 5, (9); N^{op} is the operational counting process, and ℓ^{op} is the per-event net loss after SLA-credit recoveries. The spot–credit covariance

$$
\Gamma(t,T) \;=\; \mathrm{Cov}^{\tilde{\mathbb{Q}}}\Big(\textstyle\int_t^T \lambda^{\text{term}}(s)\,ds,\; \ln \Pi^g(T)\Big)
$$

arises because the intensity and the spot share $X^{\text{supply}}, X^{\text{macro}}$ and the lifecycle state ζ. Conditional independence is the corner $\Gamma = 0$ (credit factors orthogonal to the spot), where the delivery term reduces to the familiar product $S \cdot G^g$; in general Γ is given in closed form in Section 6; as a price adjustment it scales with the default intensity, subdominant for investment-grade names and leading in the distressed regime (Section 7). Equation (1) is the framework's centerpiece; its blocks are developed

© 2026 by the author(s). Distributed under a Creative Commons CC BY license.

Preprints.org (www.preprints.org) | NOT PEER-REVIEWED | Posted: 23 June 2026 doi:10.20944/preprints202606.1651.v1

in turn: the cost-of-carry G^g and its lifecycle drift (Section 4), the two-mode credit terms (Section 5), their affine form, lifecycle coupling, and Γ-transform (Section 6), and the H100 calibration (Section 7).

Relation to CVA.

The credit adjustment $G^g - F^g - L^{\mathrm{op}}$ is a unilateral credit valuation adjustment (G^g the exposure, $1 - R$ the loss given default, Γ the spot–credit covariance correction; Hull and White [17]; Brigo et al. [20]; Ballotta et al. [27]; Ghamami and Goldberg [28]; Brigo et al. [29]; Gregory [30]), but three features take it beyond the standard construction. The exposure G^g is a non-storable, obsolescing commodity forward (Section 4), not a hedgeable mark-to-market taken as given. The credit–value coupling is *structural and physical*: the lifecycle chain (11) couples exposure and hazard — right-way on delivery, wrong-way on recovery — through hardware obsolescence itself, not a fitted correlation; unlike policy-driven firm-value stranding (Battiston et al. [31]), the shared driver is the asset's own technology cycle. And the exposure is *unspanned*, priced by local risk-minimization under the MMM (Section 6) rather than by replication.

Cost-of-carry form of G^g.

The survival-conditional forward admits the cost-of-carry exponential

$$G^g(t,T) \;=\; P^{g,\mathrm{spot}}(t)\cdot\exp\big[(r+u-q-\eta^g)(T-t)\big], \tag{2}$$

where r is the risk-free rate, q is a convenience yield (below), u is the tradeability friction (below), and η^g is the lifecycle-state-dependent technology drift (Section 4). A discrete event-premium factor $(1+Q^{\mathrm{disc}})$ aggregating governance and priority-access premia is typically ≈ 1 ($Q^{\mathrm{disc}} \ll 1$) for single-issuer pricing and is omitted here.

Carry wedges q and u.

The exponent (2) also carries a convenience yield q, the Kaldor–Working–Brennan value of holding a reserved claim rather than inventory (Kaldor [32]; Brennan [33]; Gibson and Schwartz [34]; non-storable adaptation: Lucia and Schwartz [35]; Cartea and Figueroa [36]; Davis [37]; Bessembinder and Lemmon [38]; Routledge et al. [39]), and a tradeability friction u, the per-unit-time cost of reselling the claim: $u \approx 0$ on liquid tiers, divergent ($u \to \infty$) for non-transferable contracts, where cash-and-carry breaks and (1) is indicative rather than arbitrage-enforced. Both are secondary here. Spot and forward pin only the *net* exponent $(r+u-q-\eta^g)$, so we fix η^g *ex ante* from the roadmap (the load-bearing term, which then cannot absorb the others) and, on the transferable marketplace tier, set $u \approx 0$ and fold q (financing roughly offsets it), leaving η^g as the operative carry.

Grade-vector channels.

The grade g enters (1)–(2) through three distinct channels: the spot reference $P^{g,\mathrm{spot}}$, the lifecycle-state drift η^g via the state space of Section 4, and the face value V of Section 5 (the grade-specific purchase price). Cross-grade substitution operates through workload re-architecture, not a price discount, so a deliverable-substitute approximation overstates inter-grade fungibility; cross-grade no-arbitrage is a multi-grade question beyond this single-grade treatment.

4. Lifecycle States and Roadmap-Timed Transitions

This section develops the lifecycle technology-drift η^g in the commodity forward G^g of (1). Compute productivity moves through a discrete generational lifecycle (cf. Ma [40] on obsolescence and firm value), so a forward spanning a transition cannot be priced with constant drift. We make η^g state-dependent, $\eta^g(\zeta)$, over a compact state space restricted to the *obsolescence-driven* phases at or past a successor's launch, where depreciation is structurally identifiable from roadmap cadence (Table 2). A current-generation grade with no announced successor is priced at observed spot with a

© 2026 by the author(s). Distributed under a Creative Commons CC BY license.

Preprints.org (www.preprints.org) | NOT PEER-REVIEWED | Posted: 23 June 2026 doi:10.20944/preprints202606.1651.v1

low demand-dominated baseline outside the space, entering only at successor launch: the framework prices the obsolescence-driven *shape*, not the demand-driven *level*.

Definition 2 (Lifecycle state space). *Within each architecture family, the* lifecycle state space *is the ordered set* $\mathcal{L} = \{M, C, O\}$ *of obsolescence-driven regimes:* mid-life *(*M*, the post-launch depreciation cliff),* commodity *(*C*, legacy with moderate decelerating depreciation), and* obsolete *(*O*, drifting to a salvage floor), the three post-successor phases (Figure 1); the pre-successor phases (pre-launch, premium, mainstream) are demand-driven and form the exogenous frontier baseline outside* $\mathcal{L}$*. For grade* g *at time* t*, the state* $\zeta(g,t) \in \mathcal{L}$ *is observable from market signals; transitions proceed forward only, with ambiguous assignments handled probabilistically through the transition hazard* (3).

Table 2. Within-state technology-drift anchors, each fixed from a source independent of the issuer's own forward curve, so the curve-implied drift recovered in Section 7 (Validation 2) is an *over-identifying* check rather than the calibration input (sources: SEC 10-Ks for accounting life, NVIDIA datasheets for performance-per-dollar, Silicon Data [41] for the rental decline, resale trackers for the obsolete floor). The obsolete state carries the least precise anchor and is not entered within tenor by the worked example.

State	$\eta^g(\zeta)$	Exogenous anchor (independent of the grade's forward curve)	Strength
mid-life M	$\approx 25\%/\text{yr}$	generational perf-per-dollar; rental decline of the just-superseded grade	strong
commodity C	$\approx 20\%/\text{yr}$	hyperscaler accounting useful life (5–6 yr book)	strong
obsolete O	≈ 10–$15\%/\text{yr}$	used-hardware resale residual (decelerating to a floor)	indicative

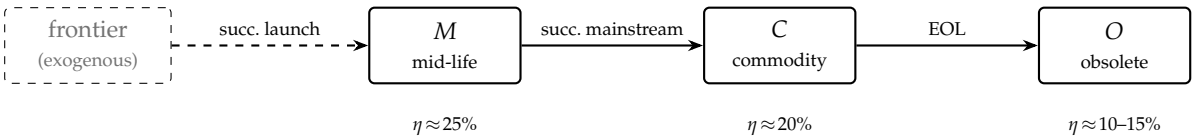

Figure 1. Three obsolescence-driven lifecycle states for a hardware grade g. The grade enters at *mid-life* when its successor launches (dashed: the pre-successor frontier period is an exogenous, demand-dominated baseline outside the state space) and transitions forward on publicly announced roadmap events. Within-state drifts $\eta^g(\zeta)$ decelerate toward a salvage floor; anchors in Table 2, calibrated values in the H100 example of Section 7.

Transition dynamics.

Transitions are partly deterministic (manufacturer roadmap cadence) and partly stochastic (timing slippage, demand shifts, supply-chain disruption), modeled through a probit hazard: the trigger is a *scheduled* event with a central expected date $\bar{T}_{\zeta\to\zeta'}$ and roughly symmetric jitter $\sigma_{\zeta\to\zeta'}$, which a memoryless exponential (modal transition at $t = 0$) cannot represent. For each transition $\zeta \to \zeta'$, with expected transition time $\bar{T}_{\zeta\to\zeta'}$ and timing uncertainty $\sigma_{\zeta\to\zeta'}$, the probability that grade g remains in state ζ at time $t > t_\zeta$ given entry at t_ζ is

$$\mathbb{P}[\zeta(g,t) = \zeta \mid t_\zeta] = 1 - \Phi\left(\frac{t - t_\zeta - \bar{T}_{\zeta\to\zeta'}}{\sigma_{\zeta\to\zeta'}}\right), \tag{3}$$

the survival function under a probit hazard, with Φ the standard normal cumulative distribution function. The state distribution $\pi_\zeta(t \mid t_0) = \mathbb{P}[\zeta(g,t) = \zeta \mid \mathcal{F}_{t_0}]$ (the occupation probability, $\sum_\zeta \pi_\zeta = 1$) follows by iterating (3) along the sequential chain $M \to C \to O$; combining with the state-dependent drift $\eta^g(\zeta)$ gives the state-conditional mixture form

$$F^g(t_0, T) \;=\; \sum_{\zeta\in\mathcal{L}} \pi_\zeta(T \mid t_0) \cdot F^g_\zeta(t_0, T), \tag{4}$$

© 2026 by the author(s). Distributed under a Creative Commons CC BY license.

Preprints.org (www.preprints.org) | NOT PEER-REVIEWED | Posted: 23 June 2026 doi:10.20944/preprints202606.1651.v1

where F^g_ζ is (1) evaluated with the within-state drift $\eta^g(\zeta)$ and within-state spot reference P^g_ζ, the sum running over $\mathcal{L} = \{M, C, O\}$. Entry into M is set by the successor's observed launch date; the two transitions within $\mathcal{L}$ carry the roadmap-cadence anchors of Table 3 (V100/A100/H100 patterns, IntuitionLabs [42]).

Table 3. Transition anchors ($\bar{T}, \sigma$ measured from entry into the originating state). Entry into M (successor launch) is observed; the pre-M frontier period is exogenous and not modelled within $\mathcal{L}$.

Transition	Trigger (roadmap event)	$\bar{T}$	σ
$M \to C$	successor reaches mainstream	30 mo	6 mo
$C \to O$	end-of-life / second successor	24 mo	6 mo

Dual role across branches.

$\zeta(g, t)$ drives both branches of (1): commodity via the drift $\eta^g(\zeta)$ in (2), and credit via an obsolescence depth $D(\zeta)$ in the bankruptcy intensity (Section 6), the flow and the stock of one process. Obsolescence is set by performance-per-watt against the frontier: each generation improves efficiency per unit compute by roughly 2–3× on a near-annual cadence, and because power dominates datacenter operating cost, an older grade turns uneconomic for frontier work within 18–36 months [43]. We define $D : \mathcal{L} \to [0, 1]$ as the normalized cumulative obsolescence of state ζ, the stock whose instantaneous rate is $\eta^g(\zeta)$: $D = 0$ at the frontier and $D(O) = 1$ at the salvage floor. Writing $H_\zeta = \sum_{\zeta' \prec \zeta} \eta^g(\zeta')\, \bar{T}_{\zeta'}$ for the drift accrued before state ζ ($\bar{T}_\zeta$ the sojourn of Table 3), the transient depths are the mid-sojourn fractions of the descent to the floor H_O,

$$D(\zeta) \;=\; \frac{H_\zeta + \frac{1}{2}\,\eta^g(\zeta)\,\bar{T}_\zeta}{H_O}, \quad \zeta \in \{M, C\}, \qquad D(O) = 1, \tag{5}$$

the best single representative of the depth accrued while in each state. With $\eta^g(M, C) = (0.25, 0.20)/\text{yr}$ and sojourns $(2.5, 2.0)$ yr, $H_C = 0.625$ and $H_O = 1.025$, so $D(M) \approx 0.30$ and $D(C) \approx 0.80$. Thus D is read from the roadmap, not chosen.

Anchoring obsolescence to perf-per-watt rather than to the rental price is deliberate: the H100 rental decline over the window was driven substantially by oversupply rather than obsolescence [41,44], while obsolescence proper redeploys capacity from training to inference, eroding revenue (price times utilization) and hardware collateral as the grade ages [45,46]. The perf-per-watt clock is roadmap-pinned and supply-free, so the credit–value coupling it induces is fixed *ex ante*. Because each drift in Table 2 is anchored to data disjoint from the grade's own forward curve, the curve-implied $\hat{\eta}_{\text{eff}}$ recovered in Section 7 is an *over-identifying restriction*, and since D is the stock of η the same check validates the depth.

5. Two-Mode Failure with Cause-Conditional Recovery

This section develops the credit blocks of (1) — the survival probability S and the loss terms L^{recovery} and L^{op}. These are the *defaultable* half of the defaultable-commodity framework, complementing the non-storable commodity branch G^g. A bond's credit risk reduces to a single binary default outcome. A compute capacity contract is exposed to two structurally distinct modes: *operational failures* (SLA breaches, partial-delivery shortfalls) partially recoverable through capped SLA credits, and *terminal failures* that end the contract, each cause carrying a distinct recovery profile (Table 4; competing-risks extension of reduced-form credit pricing, Bielecki and Rutkowski [26]). The 2022–2025 record supports this: specialized neoclouds operated continuously through H100 spot-rate volatility while mining-pivot operators experienced terminal failures (Compute North Holdings, Inc. [47]; Core Scientific, Inc. [48]); operational failures occurred in both groups without triggering terminal events.

© 2026 by the author(s). Distributed under a Creative Commons CC BY license.

Preprints.org (www.preprints.org) | NOT PEER-REVIEWED | Posted: 23 June 2026 doi:10.20944/preprints202606.1651.v1

Terminal failure with gated operational process.

Under $\tilde{\mathbb{Q}}$, the terminal failure is a totally inaccessible stopping time τ^{term} with intensity $\lambda^{\text{term}}(t) \geq 0$ adapted to the natural filtration. Under the doubly-stochastic Cox construction (Lando [15]; Bielecki and Rutkowski [26]), the survival probability admits

$$S(t,T) = \mathbb{E}^{\tilde{\mathbb{Q}}}\left[\exp\left(-\int_t^T \lambda^{\text{term}}(s)\, ds\right) \middle| \mathcal{F}_t\right]. \tag{6}$$

Operational failure events follow a Cox process $N^{\text{op}}(t)$ with $\tilde{\mathbb{Q}}$-intensity $\lambda^{\text{op}}(t) \cdot \mathbf{1}_{\{t<\tau^{\text{term}}\}}$, where the indicator gates the intensity off after the terminal event: terminal is *absorbing* (the first occurrence ends the contract) while operational is *recurrent* (multiple events possible during the survival period). Each event produces net loss $\ell^{\text{op}}(s)$ after capped SLA-credit recoveries (e.g., AWS Service Credits at 10–25% monthly fees, CoreWeave prorated refunds, and DePIN slashing bounded by staked pool). The expected operational loss takes the compensator form

$$L^{\text{op}}(t,T) = \mathbb{E}^{\tilde{\mathbb{Q}}}\left[\int_t^{T\wedge\tau^{\text{term}}} B(t,s)\, \ell^{\text{op}}(s)\, \lambda^{\text{op}}(s)\, ds \middle| \mathcal{F}_t\right]. \tag{7}$$

We take the severity ℓ^{op} deterministic, so the operational stream needs no separate spot–credit correction; a spot-dependent severity would be quadratic in the state, handled as the recovery stream is in Remark 4.

Cause-conditional intensity decomposition.

Terminal failure resolves into competing causes. Each cause κ carries a first-jump intensity $\lambda^{(\kappa)}(t) \geq 0$ and a Cox stopping time $\tau^{(\kappa)}$—the first instant the integrated cause-κ intensity crosses an independent unit-exponential threshold, exactly as τ^{term} arises from λ^{term} (Section 3). Terminal failure is the earliest cause to fire, $\tau^{\text{term}} = \min_\kappa \tau^{(\kappa)}$; because the cause thresholds are independent, survival factorizes across causes and the intensities add,

$$\lambda^{\text{term}}(t) = \sum_\kappa \lambda^{(\kappa)}(t), \tag{8}$$

with the cause-κ intensities conditionally independent given the state-factor path. Seven sub-causes organize the decomposition empirically, summarized in Table 4. The expected recovery in (1) sums over the cause that ends the contract, with cause-conditional recovery rate $R^{(\kappa)} \in [0,1]$ applied to the fixed face value V:

$$L^{\text{recovery}}(t,T) = \sum_\kappa \mathbb{E}^{\tilde{\mathbb{Q}}}\left[\mathbf{1}_{\{\tau^{(\kappa)}=\tau^{\text{term}},\, \tau^{\text{term}}\leq T\}}\, B(t,\tau^{\text{term}})\, R^{(\kappa)}\, V \middle| \mathcal{F}_t\right]. \tag{9}$$

© 2026 by the author(s). Distributed under a Creative Commons CC BY license.

Preprints.org (www.preprints.org) | NOT PEER-REVIEWED | Posted: 23 June 2026 doi:10.20944/preprints202606.1651.v1

Table 4. Sub-causes and recovery regimes. Non-bankruptcy empirical anchors: force majeure (Texas grid 2021, Hurricane Beryl 2024; $R \approx 0$); regulatory (US export controls 2022–2025; $R \approx 0$); ecosystem (Terra/Luna 2022; $R < 0.10$); acquisition (2024 DC-portfolio M&A; $R \approx 1$).

Cause κ	Mechanism	Recovery regime
Bankruptcy (bk)	Insolvency via revenue collapse, debt distress, capital-flight cascade	Stochastic estate distribution; $R \in [0.30, 0.50]$, downturn-LGD correlated
Force majeure (fm)	Disaster, cyber attack, civil-authority order, sanctions equipment block, upstream grid collapse	$R \approx 0$ by standard SLA exclusion
Regulatory shutdown (rs)	Export-control revocation, sanctions, agency-ordered termination	$R \approx 0$; voided by government action
Acquisition · assumption (aa)	Acquirer assumes contract at original terms	$R \approx 1.0$ via successor entity
Acquisition · repudiation (ar)	Acquirer declines; contract becomes residual claim	$R \in [0.20, 0.60]$; acquirer discretion, creditor priority
Ecosystem collapse (ec)	Issuer survives but supporting ecosystem ceases delivery	$R \in [0, 0.30]$; higher if distributed operators persist
Verifiability dispute (vd)	Issuer survives but SLA enforcement fails (measurement, arbitration)	Case-specific via dispute mechanism

Remark 1 (Recovery of Face Value)**.** *The face value V is the contract's purchase price (e.g., CoreWeave Order Form prepaid amount, AWS Capacity Blocks fee, and DePIN staked reference), priced under Recovery-of-Face-Value (Duffie [49]; cf. Jarrow and Turnbull [50]), distinct from the Recovery of Market Value of Duffie and Singleton [25]. RFV fits compute contracts: recovery clauses are denominated in fractions of purchase price, it has corporate-bond support (Berd et al. [51]; Casas Vivas [52]), and it avoids RMV's "market value of an illiquid contract" issue.*

Each $\lambda^{(\kappa)}$ loads on different state factors (bankruptcy on macro credit and idiosyncratic health, regulatory on jurisdictional exposure, force majeure on common shocks), and $R^{(\mathrm{bk})}$ shares the macro factors of $\lambda^{(\mathrm{bk})}$ (the downturn-LGD channel), inducing λ–R correlation. The Biagini–Cretarola structure condition holds: the spot's market price of risk has finite mean-variance tradeoff over the finite tenor, so the $\tilde{\mathbb{Q}}$-density is a true martingale, and the default, recovery, and operational martingales are orthogonal to the spot Brownian under the Cox construction, leaving them unpriced.

Remark 2 (Wrong-way recovery covariance)**.** *Bankruptcy intensity and bankruptcy recovery share common-factor loadings:*

$$\mathrm{Cov}^{\tilde{\mathbb{Q}}}\big[\lambda^{(bk)}(t),\, R^{(bk)}(t) \,\big|\, \mathcal{F}_0\big] \;=\; \mathbf{a}^{(bk)\top}\, \boldsymbol{\Sigma}_X(t)\, \mathbf{r}^{(bk)}, \tag{10}$$

where $\mathbf{r}^{(bk)}$ is the factor loading of $R^{(bk)}$ on $\mathbf{X}_t$ and $\boldsymbol{\Sigma}_X(t)$ is the factor covariance. Negative covariance signals wrong-way risk: bad states (high λ) coincide with low recoveries.

6. Affine Intensity, the Joint Spot–Credit Transform, and Lifecycle Coupling

This section casts the survival probability S of (1) in closed affine form, couples the lifecycle state to the bankruptcy intensity, and derives the Föllmer–Schweizer hedge. The cause-specific intensities $\{\lambda^{(\kappa)}\}_\kappa$ and operational intensity λ^{op} are affine under $\tilde{\mathbb{Q}}$, delivering closed-form survival via affine transform (Duffie et al. [16]). The affine form is the leading-order specification — the linearization of any smooth factor–intensity map, with the quadratic-affine extension (Cheng and Scaillet [53]) the principled next order, invoked only when curvature is identifiable — and it is the maximal class for which the pricing transform stays exponential-affine, so the survival, the spot–credit correction Γ, and the hedge all inherit closed forms.

© 2026 by the author(s). Distributed under a Creative Commons CC BY license.

Preprints.org (www.preprints.org) | NOT PEER-REVIEWED | Posted: 23 June 2026 doi:10.20944/preprints202606.1651.v1

6.1. Intensity Dynamics and Closed-Form Survival

Factor state.

The joint state stacks common and idiosyncratic factors: $\mathbf{Z}_t = (\mathbf{X}_t, Y^{\text{op}}, Y^{\text{term}})$, where $\mathbf{X}_t = (X^{\text{supply}}, X^{\text{macro}}, X^{\text{infra}}, X^{\text{reg}})$ captures supply, macro, infrastructure, and regulatory stress. Non-negative components follow CIR (Cox et al. [54]); naturally-signed components follow Vasicek (Vasicek [55]). Idiosyncratic $Y^{(\cdot)}$ follow CIR. The joint dynamics are affine,

$$d\mathbf{Z}_t = \mathbf{K}(\boldsymbol{\theta} - \mathbf{Z}_t)\, dt + \left(\boldsymbol{\Sigma}_0 + \boldsymbol{\Sigma}_1 \mathbf{Z}_t\right)^{1/2} d\mathbf{W}_t,$$

with mean-reversion speeds $\mathbf{K}$, long-run means $\boldsymbol{\theta}$, and instantaneous covariance affine in the state: the Vasicek (Gaussian) components contribute the constant part $\boldsymbol{\Sigma}_0$, the CIR components the state-scaled part $\boldsymbol{\Sigma}_1$. The parameters $(\mathbf{K}, \boldsymbol{\theta}, \boldsymbol{\Sigma}_0, \boldsymbol{\Sigma}_1)$ are calibrated to the factor series (Section 7).

Affine intensity map.

The operational intensity and the terminal-cause intensities other than bankruptcy are affine in the state,

$$\begin{aligned}
\lambda^{\text{op}}(t) &= a_0^{\text{op}} + \mathbf{a}^{\text{op}\top} \mathbf{X}_t + b^{\text{op}}\, Y^{\text{op}}(t), \\
\lambda^{(\kappa)}(t) &= a_0^{(\kappa)} + \mathbf{a}^{(\kappa)\top} \mathbf{X}_t + b^{(\kappa)}\, Y^{\text{term}}(t), \quad \kappa \neq \text{bk},
\end{aligned}$$

with intercepts $a_0^{(\cdot)} \geq 0$, idiosyncratic loadings $b^{(\cdot)} \geq 0$, and common-factor loadings constrained so the affine map preserves each $\lambda^{(\cdot)} \geq 0$; the bankruptcy intensity carries an extra lifecycle term, defined next.

Lifecycle–bankruptcy coupling.

The state $\zeta(g,t)$ couples into the bankruptcy intensity through an additive covariate

$$\lambda^{(\text{bk})}(t) = a_0^{(\text{bk})} + \mathbf{a}^{(\text{bk})\top} \mathbf{X}_t + b^{(\text{bk})}\, Y^{\text{term}}(t) + \beta^{\text{lifecycle}}\, D(\zeta), \tag{11}$$

with $D(\zeta)$ the cumulative-obsolescence depth of (5) ($0 < D(M) < D(C) < D(O) = 1$). Here $\beta^{\text{lifecycle}} \geq 0$ is the issuer-specific *lifecycle–credit loading*, the sensitivity of the bankruptcy intensity to obsolescence depth. For a single issuer it is calibrated to the issuer's own credit spread (Section 7). Lifecycle stress enters through revenue (old grades priced lower) and collateral (hardware-backed debt loses value as the fleet ages); it is additive to the macro and idiosyncratic baseline $\mathbf{a}^{(\text{bk})\top}\mathbf{X}_t$ rather than an interaction with it, so downturn amplification lives in that baseline and the wrong-way recovery (Remark 4), not in the obsolescence term. Aggregating across κ via (8) yields an affine λ^{term}, with aggregate intercept $a_0^{\text{term}} = \sum_\kappa a_0^{(\kappa)}$ and aggregate loading $\mathbf{a}^{\text{term}}$ stacking $\sum_\kappa \mathbf{a}^{(\kappa)}$ on $\mathbf{X}_t$ and $\sum_\kappa b^{(\kappa)}$ on Y^{term} (zero on Y^{op}); the lifecycle term $\beta^{\text{lifecycle}} D(\zeta)$ is a state-conditional intercept carried by the regime system (23), not by a_0^{term}.

Closed-form survival.

Under this specification, the survival probability (6) admits the closed-form exponential-affine expression

$$S(t,T) = \exp\left(A^S(\tau) + \mathbf{B}^S(\tau)^\top \mathbf{Z}_t\right), \quad \tau = T - t, \tag{12}$$

with $A^S(0) = 0$ and $\mathbf{B}^S(0) = \mathbf{0}$ satisfying the Riccati system:

$$\begin{aligned}
\frac{dA^S}{d\tau} &= -a_0^{\text{term}} + \mathbf{B}^{S\top}(\mathbf{K}\boldsymbol{\theta}) + \tfrac{1}{2}\, \mathbf{B}^{S\top} \boldsymbol{\Sigma}_0\, \mathbf{B}^S, \\
\frac{d\mathbf{B}^S}{d\tau} &= -\mathbf{a}^{\text{term}} - \mathbf{K}^\top \mathbf{B}^S + \tfrac{1}{2}\, \mathbf{B}^{S\top} \boldsymbol{\Sigma}_1\, \mathbf{B}^S,
\end{aligned} \tag{13}$$

© 2026 by the author(s). Distributed under a Creative Commons CC BY license.

Preprints.org (www.preprints.org) | NOT PEER-REVIEWED | Posted: 23 June 2026 doi:10.20944/preprints202606.1651.v1

where $(\mathbf{K}, \boldsymbol{\theta})$ are $\mathbf{Z}_t$ mean-reversion parameters and $(\boldsymbol{\Sigma}_0, \boldsymbol{\Sigma}_1)$ separate state-independent and state-dependent diffusion (the last $\mathbf{B}^S$ term is component-wise). The system is the standard affine reduction — substitute the exponential-affine ansatz (12) into the Feynman–Kac equation for S and match coefficients in $\mathbf{Z}_t$ — with existence and uniqueness on multi-year tenors at typical calibrations from Duffie et al. [16]. Here (13) is the baseline (lifecycle-free) survival; the lifecycle-coupled form is the regime system (23), which with all couplings off ($\beta^{\text{lifecycle}} = 0$, no common shocks, a single cause) collapses to the Lando [15] closed-form. The operational loss L^{op} (7) and the cause-conditional recovery L^{recovery} (9) admit parallel exponential-affine forms via the same machinery; substitution into (1) yields tractable $F^g(t, T)$.

6.2. Hedging and the Joint Spot–Credit Transform

The last subsection fixed the credit side — the affine intensity, its lifecycle coupling, and the closed-form survival S that feeds the delivery term $S\,G^g$ of (1). Now we turn to the spot–credit interaction, which surfaces at two orders: the Föllmer–Schweizer hedge ratio ξ^{FS} carries it at first order (an $O(1)$ covariation beta), while the joint spot–credit transform delivers the level correction Γ at second order (the $O(\sigma^2)$ factor $e^{-\Gamma}$). One may thus price as if spot and credit were conditionally independent (the factorization of Section 3) but must not hedge that way.

Föllmer–Schweizer hedge ratio.

The Föllmer–Schweizer decomposition (Föllmer and Schweizer [12]) extended to defaultable claims by Biagini and Cretarola [13] writes the payoff as

$$F^g(T) = F^g(t) + \int_t^T \xi_s^{FS}\, dP^{g,\text{spot}}(s) + L^{FS}(T) - L^{FS}(t), \quad \xi^{FS}\ \mathbb{F}\text{-predictable}, \ \ L^{FS} \perp P^{g,\text{spot}}. \tag{14}$$

ξ^{FS} is the predictable covariation ratio $d\langle F^g, P^{g,\text{spot}}\rangle_t / d\langle P^{g,\text{spot}}\rangle_t$ under the minimal martingale measure $\tilde{\mathbb{Q}}$ of Föllmer and Schweizer [12]; this ratio is the variance-minimizing hedge. The partial-derivative representation below holds for continuous-spot Markovian dynamics (the spot's jump components feed L^{FS}). Differentiating (1) under the cost-of-carry form, holding (u, q, η^g) fixed at current state ($\partial G^g / \partial P^{g,\text{spot}} = G^g / P^{g,\text{spot}}$),

$$\xi_t^{FS} \;=\; \frac{\partial F^g}{\partial P^{g,\text{spot}}} \;=\; S(t,T)\,\frac{G^g(t,T)}{P^{g,\text{spot}}(t)} \;+\; \underbrace{\frac{\partial (L^{\text{recovery}} - L^{\text{op}})}{\partial P^{g,\text{spot}}}}_{\text{via } (\mathbf{X}_t, Y^{\text{term}}) \text{ co-movement}}. \tag{15}$$

The bracketed channel is *spanned* but not negligible — X_t^{supply}, X_t^{macro}, and the lifecycle state $\zeta(g,t)$ all co-move with $P^{g,\text{spot}}$, an $O(1)$ sensitivity the hedge must carry. Keeping only the leading multiplicative term gives

$$\xi_t^{FS} \;\approx\; S(t,T)\,\frac{G^g(t,T)}{P^{g,\text{spot}}(t)} \;=\; \frac{F^g(t,T) - L^{\text{recovery}}(t,T) + L^{\text{op}}(t,T)}{P^{g,\text{spot}}(t)}. \tag{16}$$

The two reductions differ in status. The pieces (16) drops — the bracketed channel and the held-fixed spot-comovement of (u, q, η^g) — are *spanned*, hence hedgeable: discarding them is hedge-ratio error, not irreducible risk, and "hedging as though spot and credit were independent" is exactly stopping at (16). What is genuinely *unspanned* is collected in L^{FS} — idiosyncratic intensity, Marshall–Olkin default jumps, lifecycle-transition jumps, and the unspanned part of recovery (wrong-way per Remark 2) — the irreducible incompleteness the minimal martingale measure leaves unpriced. Operationally the desk holds $\xi^{FS} \approx 0.5$ units of rental spot per unit of contract (survival times the carry ratio $G^g / P^{g,\text{spot}}$, each below one; the H100 value is calibrated in Section 7), carrying the bracketed channel up toward the full (15), and bears L^{FS} unhedged. The spanned correction is bounded by the state-conditional spread, $\xi_t^{FS} \in [0.50, 0.58]$ across lifecycle states (a $\pm 16\%$ band, Section 7), with (16) the 0.50 floor.

© 2026 by the author(s). Distributed under a Creative Commons CC BY license.

Preprints.org (www.preprints.org) | NOT PEER-REVIEWED | Posted: 23 June 2026 doi:10.20944/preprints202606.1651.v1

The joint spot–credit transform and the correction Γ.

The transform is built from three ingredients — the object Ψ, the pricing measure, and an augmented state — assembled in Proposition 1 (with Γ specialized to a single factor in Remark 3). The delivery term $S\,G^g e^{-\Gamma}$ of (1) is the survival-weighted delivery

$$\Psi(t,T) := \mathbb{E}^{\tilde{\mathbb{Q}}}\big[\mathbf{1}_{\{\tau^{\text{term}}>T\}}\, B(t,T)\,\Pi^g(T) \mid \mathcal{F}_t\big].$$

Ψ and the correction Γ follow from the same affine machinery as the survival S above. The affine intensity map loads $\lambda^{(\kappa)}$ on the same $X^{\text{supply}}, X^{\text{macro}}$ that drive the spot $P^{g,\text{spot}}$, and the lifecycle state ζ couples both branches through (11), so conditional independence ($\Gamma = 0$) would require an orthogonality the framework's own structure precludes.

The pricing measure under correlation.

The minimal martingale measure has density $\mathcal{E}(-\int_0^T \theta_s\, dW_s)$ (Section 5), built only from the tradeable spot's Brownian W and its market price of risk $\theta_t = (\mu_t - r)/\sigma_t$. By Girsanov, a common factor with $d\langle W^j, W\rangle = \varrho_j\, dt$ acquires under $\tilde{\mathbb{Q}}$ the re-drift

$$\theta^{j,\tilde{\mathbb{Q}}} \;=\; \theta^{j,\mathbb{P}} \;-\; \frac{\sigma^j\,\varrho_j\,\theta_t}{K_j}, \qquad j \in \{\text{macro}, \text{reg}\}, \tag{17}$$

with K_j the factor's mean-reversion rate and ϱ_j the spot–factor correlation (distinct from the continuity-premium ratio $\rho \equiv F^g/G^g$); the CIR components carry the analogous essentially-affine adjustment (Duffee [56]). The same ϱ_j that breaks conditional independence sets how much of the spot's risk premium the measure imputes to the credit factors, so covariance and re-drifting are one parameter: at $\varrho_j = 0$ the factors are orthogonal and unpriced, the regime Section 3–Section 7 operate in.

Augmented state.

Promote the log-spot to a state coordinate,

$$Y^P(t) := \ln P^{g,\text{spot}}(t), \qquad \mathbf{Z}_t = (\mathbf{X}_t,\, Y^{\text{op}},\, Y^{\text{term}},\, Y^P), \tag{18}$$

with $\tilde{\mathbb{Q}}$-dynamics

$$dY^P = \big(r + u - q - \eta^g(\zeta) - \tfrac{1}{2}\sigma_P^2\big)\,dt + \sigma_P\, dW,$$

so that $\mathbb{E}^{\tilde{\mathbb{Q}}}[P^{g,\text{spot}}(T) \mid \mathcal{F}_t]$ recovers the cost-of-carry forward (2). Correlation enters only through the spot–factor diffusion blocks $\Sigma_{Pj} = \sigma_P\,\sigma^j\,\varrho_j$; the intensity map does *not* load on Y^P (default responds to stress, not price level), and conditional independence (Section 3) is exactly $\Sigma_{Pj} = 0$.

Proposition 1 (Joint spot–credit transform). *The delivery stream Ψ of (1) admits the exponential-affine form*

$$\Psi(t,T) = \exp\big(A^\Psi(\tau) + \mathbf{B}^\Psi(\tau)^\top\,\mathbf{Z}_t\big), \tag{19}$$

where $(A^\Psi, \mathbf{B}^\Psi)$ solve the Riccati system (13) on the augmented state (18), with the discount r added to the A-intercept, making it $r + a_0^{term}$, under the single changed boundary condition

$$\mathbf{B}^S(0) = \mathbf{0}\ \textit{(survival)} \qquad \textit{versus} \qquad \mathbf{B}^\Psi(0) = \mathbf{e}_{Y^P}\ \textit{(delivery)}, \tag{20}$$

the unit vector on the log-spot coordinate, supplied by the payoff $\Pi^g(T) = e^{Y^P(T)}$, and $A^\Psi(0) = 0$. The spot–credit covariance is carried by the quadratic term $\frac{1}{2}\,\mathbf{B}^{\Psi\top}\boldsymbol{\Sigma}\,\mathbf{B}^\Psi$, with $\boldsymbol{\Sigma} = \boldsymbol{\Sigma}_0 + \boldsymbol{\Sigma}_1\mathbf{Z}_t$ the augmented-state covariance: the Y^P-component of $\mathbf{B}^\Psi$ (equal to 1 at $\tau = 0$) couples to the $\mathbf{X}$-components through the off-diagonals Σ_{Pj}. When $\Sigma_{Pj} = 0$ the Y^P block decouples and (19) factors as $S \cdot G^g$, the delivery term of (1) at the conditional-independence corner $\Gamma = 0$.

© 2026 by the author(s). Distributed under a Creative Commons CC BY license.

Preprints.org (www.preprints.org) | NOT PEER-REVIEWED | Posted: 23 June 2026 doi:10.20944/preprints202606.1651.v1

The proof is the affine reduction of Duffie et al. [16]: the ansatz (19) substituted into the Feynman–Kac equation for $\mathbb{E}[e^{-\int_t^T (r+\lambda^{\text{term}})ds}\, e^{Y^P(T)}]$ and matched in $\mathbf{Z}_t$. The two transforms share the $\mathbf{B}$-equation of (13); only their terminal condition (20) differs.

Remark 3 (The conditional-independence correction as a single factor). *For Gaussian factors, $(\Lambda, Y^P(T))$ with $\Lambda = \int_t^T \lambda^{term}(s)\, ds$ is jointly Gaussian under $\tilde{\mathbb{Q}}$ and (19) reads*

$$\Psi(t,T) \;=\; S(t,T)\cdot G^g(t,T)\cdot \exp\big(-\mathrm{Cov}^{\tilde{\mathbb{Q}}}(\Lambda,\, Y^P(T))\big), \tag{21}$$

$$\mathrm{Cov}^{\tilde{\mathbb{Q}}}(\Lambda, Y^P(T)) = \sigma_P \sum_j a_j^{term}\, \frac{\sigma^j \varrho_j}{K_j}\Big[\tau - \frac{1-e^{-K_j\tau}}{K_j}\Big] \xrightarrow{K_j\tau \ll 1} \frac{\tau^2}{2}\,\sigma_P \sum_j a_j^{term}\,\sigma^j\varrho_j, \tag{22}$$

with a_j^{term} the j-component of the aggregate loading $\mathbf{a}^{term}$. The correction is one scalar, multiplicative, and grows quadratically in tenor. Conditional independence is the null Cov $= 0$*, a testable restriction: σ_P and the spot–factor correlations ϱ_j are estimable from the realized rental and credit series. Negative spot–credit comovement ($\varrho_j < 0$) makes* Cov < 0*, lifting the delivery stream above $S \cdot G^g$.*

Remark 4 (Wrong-way recovery). *The recovery stream carries the opposite-signed correction (terminal failures concentrate in low-spot states, the bankruptcy recovery itself wrong-way, Remark 2), but we leave $L^{recovery}$ uncorrected by design. The effect is sub-dominant in the investment-grade regime priced here (about* 1% *of F^g, Section 7), and anchoring $R^{(\kappa)}$ to* default-conditional *recoveries (senior-unsecured averages and the 2022 cohort, both over actual defaults) already embeds the downturn-LGD, so the term is approximately wrong-way-correct without a separate factor. Pricing its dynamic factor covariance endogenously would require the quadratic-affine extension (Cheng and Scaillet [53]), available but unnecessary at the present data resolution.*

The hedge ratio ξ^{FS} of (15) is the *same* correlation at first order: the level correction (21) is the $O(\sigma^2)$ covariance, while the bracketed channel of (15) is the $O(1)$ covariation beta. Spot–credit dependence is thus priced in the hedge (first order) and in the level (second order), reconciling the conditional factorization of Section 3 with the first-order comovement established above.

6.3. Full Price and Exact Lifecycle Mixing

Two threads close the section: assembling the full price, and giving the lifecycle its exact, rather than mixture-approximated, treatment — the latter, (23) below, being the joint transform of Proposition 1 lifted to a Markov chain over regimes, inheriting its augmented-state machinery and adding only the generator coupling. First, every block of (1) is the *same* exponential-affine transform read off at a different rate and boundary — S at rate λ^{term} with $\mathbf{B}(0) = \mathbf{0}$; G^g at rate r with $\mathbf{B}(0) = \mathbf{e}_{Y^P}$; Ψ at rate $r + \lambda^{\text{term}}$ with $\mathbf{B}(0) = \mathbf{e}_{Y^P}$; and L^{recovery}, L^{op} as the matching default-timing and running integrals — so the full price assembles from this one object. Second, the mixture (4) weights these by the *marginal* state probabilities, dropping the path-coupling (the intensity carries $\beta^{\text{lifecycle}} D(\zeta)$ over the whole path). Idealizing ζ as a Markov chain with generator

$$\mathbf{Q}^\zeta = \begin{pmatrix} -q_M & q_M & 0 \\ 0 & -q_C & q_C \\ 0 & 0 & 0 \end{pmatrix}, \qquad q_\zeta \approx 1/\bar{T}_{\zeta\to\zeta'},$$

restores it as the *exact* path treatment for the chain; the two sequential cadence rates q_M, q_C are read from the roadmap, and the zero bottom row makes O absorbing, so once a grade obsolesces the coupling $(\mathbf{Q}^\zeta\Psi)_O$ drops out. Write $A_\zeta, \mathbf{B}_\zeta$ for the regime-ζ transform coefficients, $\Psi_\zeta = \exp(A_\zeta + \mathbf{B}_\zeta^\top \mathbf{Z})$, and stack them as $\boldsymbol{\Psi} = (\Psi_\zeta)_{\zeta\in\mathcal{L}}$; each A_ζ solves

$$\frac{dA_\zeta}{d\tau} = -\big(r + a_0^{\text{term}} + \beta^{\text{lifecycle}} D(\zeta)\big) + \mathbf{B}_\zeta^\top(\mathbf{K}\boldsymbol{\theta}) + \tfrac{1}{2}\,\mathbf{B}_\zeta^\top \boldsymbol{\Sigma}_0\, \mathbf{B}_\zeta + \frac{(\mathbf{Q}^\zeta\boldsymbol{\Psi})_\zeta}{\Psi_\zeta}, \tag{23}$$

© 2026 by the author(s). Distributed under a Creative Commons CC BY license.

Preprints.org (www.preprints.org) | NOT PEER-REVIEWED | Posted: 23 June 2026 doi:10.20944/preprints202606.1651.v1

the obsolescence entering through $\beta^{\text{lifecycle}} D(\zeta)$ and the last term the ζ-row of the generator acting on the transform stack, $(\mathbf{Q}^{\zeta}\boldsymbol{\Psi})_{\zeta} = \sum_{\zeta'} Q^{\zeta}_{\zeta\zeta'} \Psi_{\zeta'}$; $\mathbf{B}_{\zeta}$ solves the $\mathbf{B}$-equation of (13). This Markov idealization smooths the scheduled probit transitions (3), whose age-dependence is a further refinement negligible at the horizons priced here.

At the H100 horizon of Section 7 the system collapses to the marginal mixture (4): the $M \to C$ transition falls past delivery ($\bar{T} = 30$ mo against a 24-month tenor), so the grade occupies essentially one state over the whole tenor; the terminal occupancy π_{ζ} that (4) weights by then already encodes the near-constant path, and the generator coupling — the only thing (23) adds beyond that marginal — is negligible. The full path treatment becomes first-order only when transitions fall inside the tenor (deep obsolescence, or the distressed regime).

7. Worked Example: H100 Forward Through Lifecycle Transition

We exercise the lifecycle states of Section 4 on an H100 forward spanning the H100 → B200 transition, anchoring all parameters to the Silicon Data H100 marketplace tier (the public series with the most consistent monthly methodology over the window). The rental market splits into a competitive *marketplace* tier (our anchor: the $u \approx 0$, transferable, arbitrage-enforced regime of Section 3), a higher *neocloud* tier, and an administered *on-demand* tier, distinct from the grade's service tier (Section 2).

Setup.

At t_0 = Q4 2024, H100 enters mid-life (M) as B200 begins volume shipping. **Anchor spot**: Silicon Data H100 2024 H2 marketplace median $\bar{P}^{g}_{M}(t_0) = \$2.58/\text{hr}$ (Silicon Data [41]); forward delivery T_3 = Q4 2026 (24-month tenor). **Drift anchors** (exogenous, Table 2): $\eta^{g}(M) \approx 25\%/\text{yr}$, $\eta^{g}(C) = 20\%/\text{yr}$; the raw 2024 H2–2025 H2 endpoint ratio \$2.58 → \$1.95 gives a ∼28%/yr *realized* rate (the V2 over-identifying check). **Transition anchor**: $M \to C$ at $\bar{T} = 30$ mo, $\sigma = 6$ mo (IntuitionLabs [42]). **State multiplier** $m_C/m_M = 0.6$ — the within-state spot scales as $P^{g}_{C} = 0.6\, P^{g}_{M} = \$1.55/\text{hr}$. **Scope**: marketplace/cohort-median tiers, grade at or past mid-life.

Commodity-branch prediction.

The state distribution at $T_3 = 24$ mo is $\pi_M = 0.84$, $\pi_C = 0.16$. Within-state forwards $F^{g}_{M}(t_0, T_3) = \$2.58 \cdot e^{-0.25 \cdot 2} \approx \$1.57/\text{hr}$ and $F^{g}_{C}(t_0, T_3) = \$1.55 \cdot e^{-0.20 \cdot 2} \approx \$1.04/\text{hr}$ give the state-weighted commodity-branch forward $G^{g}(t_0, T_3) \approx \$1.49/\text{hr}$ via (4).

Credit-branch contributions.

Anchoring to CoreWeave, a large-cap specialized neocloud (Fitch BB-/RR4 on the 9.25% 2030 senior unsecured notes, Z-spread ≈ 454 bp; Fitch Ratings [57]; BondbloX [58]), implied $\lambda^{\text{term}} \approx 0.07/\text{yr}$ at $R^{(\text{bk})} = 0.35$ (Moody's senior-unsecured 5-year average, Moody's Investors Service [59]). With $V^{(\text{bk})} = \$2.58/\text{hr}$ (RFV upper bound; actual prepaid amount typically 15–25% below spot, moving F^{g} by $\sim -2\%$), $S(t_0, T_3) \approx 0.869$; $\lambda^{\text{op}} \approx 0.10/\text{yr}$ with $\ell^{\text{op}} \approx \$0.20/\text{hr}$-equivalent (consistent with CoreWeave's prorated-refund schedule and the AWS EC2 tier benchmark for moderate outages, Amazon Web Services [60]) yields $L^{\text{op}}(t_0, T_3) \approx \$0.04/\text{hr}$; bankruptcy recovery plus near-zero force-majeure/regulatory contributions give $L^{\text{recovery}}(t_0, T_3) \approx \$0.12/\text{hr}$ (the recovery-of-face-value bound $R^{(\text{bk})} V (1 - S)$ at the senior-unsecured $R^{(\text{bk})} = 0.35$, consistent with the rate used to imply λ). The credit-adjusted forward is

$$F^{g}(t_0, T_3) \;=\; S\, G^{g} + L^{\text{recovery}} - L^{\text{op}} \;\approx\; 0.869 \times \$1.49 + \$0.12 - \$0.04 \;\approx\; \$1.37/\text{hr}. \tag{24}$$

Spot–credit correction.

Equation (24) reports the leading product $S \cdot G^{g}$ (the $\Gamma = 0$ term of (1)); we now evaluate the correction $e^{-\Gamma}$ of Section 6. Calibrating the spot–credit inputs to the marketplace tier — realized rental log-volatility $\sigma_P \approx 0.35/\text{yr}$, cumulative-hazard volatility $\sigma_\Lambda \approx 0.035$ over the 24-month tenor, and

© 2026 by the author(s). Distributed under a Creative Commons CC BY license.

Preprints.org (www.preprints.org) | NOT PEER-REVIEWED | Posted: 23 June 2026 doi:10.20944/preprints202606.1651.v1

a negative spot–credit correlation $\varrho_{\Lambda,Y} \approx -0.4$ (capacity glut and funding stress depress the rental and lift the intensity together) — the delivery-stream factor of (21) is $\exp(-\varrho_{\Lambda,Y}\,\sigma_\Lambda\,\sigma_P\sqrt{\tau}) \approx e^{+0.007}$, lifting $S\,G^g$ from \$1.295 to \$1.304 (+0.7%). The recovery stream moves the opposite way (Remark 4): a downturn-LGD haircut of order 10% lowers L^{recovery} from \$0.12 to ≈ \$0.11. The two nearly cancel, leaving $F^g \approx$ \$1.37 to within −0.2%, inside the ±5% credit-cohort band. The cancellation is structural: under negative spot–credit comovement the long gains on delivery (foregone deliveries fall in cheap-capacity states) and loses on recovery (those failures recover poorly). Conditional independence is therefore safe here demonstrably, not by assumption, but becomes leading and ceases to cancel in the distressed 2022 cohort, the regime of the multi-issuer companion (Cao and Huang [21]).

Parallel calibration: Applied Digital.

Substituting Applied Digital's anchor ($\lambda^{(\text{term})} \approx 0.13$/yr, implied by its 9.25% senior secured notes due 2030 priced at 97 (∼580 bp) via $\lambda = \text{spread}/(1-R)$ at a *secured* recovery $R \approx 0.55$ — distinct from the senior-unsecured $R = 0.35$ used for CoreWeave; Applied Digital Corporation [61]) into (24): $S \approx 0.77$, $L^{\text{recovery}} \approx$ \$0.33, $L^{\text{op}} \approx$ \$0.04, $F^g \approx$ \$1.43/hr: Applied Digital's higher intensity ($\lambda \approx 0.13$ vs 0.07) is *more* than offset by its secured recovery ($R \approx 0.55$ vs 0.35), so it prices slightly *above* unsecured CoreWeave despite the wider spread — the framework netting recovery against intensity rather than reading the spread alone. The Föllmer–Schweizer cross-tier hedge (25) transfers via the same $\beta_{\phi|P}$.

Lifecycle–credit coupling for the single issuer.

The CoreWeave spread pins the loading at mid-life through (11): against a diversified baseline $a_0^{(\text{bk})} \approx 0.02$ (Table 5) and $D(M) \approx 0.30$, the obsolescence increment is $\beta^{\text{lifecycle}} D(M) = 0.07 - 0.02 = 0.05$ ($\beta^{\text{lifecycle}} \approx 0.17$), scaling by the depth ratio to $0.05\,D(C)/D(M) \approx 0.13$ at end-of-life, so $\lambda^{(\text{bk})}$ rises from 0.07 to ≈ 0.15 as the grade ages. Carrying this rising intensity through the probit occupancy (3) (expected time-in-M of 23.4 of 24 months, the $M \to C$ transition lying beyond the tenor at $\bar{T} = 30$ mo) gives a cumulative hazard 0.144 against 0.140 at constant intensity, so S falls from 0.869 to 0.866 and F^g by ≈ 0.4%, within the credit-cohort band — the within-state intercept shift $\beta^{\text{lifecycle}} D(M)$ alone, the generator coupling of (23) being negligible at this horizon (Section 6). The within-issuer coupling is thus second-order at mid-life, becoming first-order only deep in obsolescence (older grades, longer tenors, or the distressed 2022 cohort), the regime of the multi-issuer companion (Cao and Huang [21]).

Per-issuer credit-spread sample.

A hedge book operates across the cohort. Table 5 samples named US-listed compute issuers with public credit data, plus the AAA/AA hyperscaler-parent benchmark.

© 2026 by the author(s). Distributed under a Creative Commons CC BY license.

Preprints.org (www.preprints.org) | NOT PEER-REVIEWED | Posted: 23 June 2026 doi:10.20944/preprints202606.1651.v1

Table 5. Per-issuer credit-anchor sample with public data sources (SEC EDGAR; FINRA TRACE; rating-agency press releases). CoreWeave provides the central single-name secondary-market anchor. †Hut 8's anchor is its ring-fenced River Bend project-finance note (BBB-, bankruptcy-remote SPV backed by a hyperscaler-linked lease); its ∼0.003 intensity reflects that lease-backed structure and *understates* Hut 8 Corp parent and compute-delivery risk.

Issuer	Credit anchor	Public source	λ^{term}
AWS, GCP, Azure	AAA/AA parent sr unsec	Issuer-parent benchmarks	0.005–0.015
CoreWeave	Fitch BB-/RR4; 9.25% 2030 Z-spread ∼454 bp	Fitch Ratings [57]; BondbloX [58]; TRACE	0.07
Nebius	Equity-implied via Merton	SEC 20-F/6-F; equity vol	0.04–0.08
Hut 8	6.192% sr secured 2042; BBB- (IG)†	PR; SEC; S&P/Fitch	∼0.003
Applied Digital	9.25% sr secured 2030 at 97; ∼580 bp impl.	Applied Digital Corporation [61]; SEC 8-K; TRACE	0.12–0.15
Core Scientific (post-emergence)	7.75% sr secured 2031; B+/S&P (2026)	SEC; S&P; TRACE	0.08–0.13

Implied λ^{term} values use standard Z-spread $/(1-R)$ for FINRA-traded bonds and Merton-style equity-implied default for equity-only issuers (Lando [15] for the reduced-form mapping). Cross-sectional λ^{term} spans $\sim$ 0.005 (hyperscaler parents) to $\sim$ 0.15 (Applied Digital), with Hut 8's ring-fenced project notes a special investment-grade case at $\sim$ 0.003. At fixed unsecured recovery $R = 0.35$, sweeping $\lambda \in [0.05, 0.15]$ ranges $F^{g}(t_0, T_3)$ over [\$1.30, \$1.40] around the CoreWeave-anchored \$1.37 (higher λ reduces S but raises L^{recovery}, partially offsetting); letting recovery instead track seniority makes the per-issuer forwards non-monotone in the spread (Table 6). The ∼19% cross-tier basis remains the dominant pricing-uncertainty channel.

Per-issuer forwards across the cohort.

Because the commodity branch G^{g}, the face V, and the operational leg are issuer-agnostic (Section 5), each named issuer's forward follows from its own intensity and seniority-implied recovery alone. The band is tight — F^{g} spans \$1.37–\$1.45, about 5% — so the commodity branch dominates and credit is a modest modifier. More telling, F^{g} is *not* monotone in the spread: the lowest forwards are the *unsecured* neoclouds (CoreWeave \$1.37, Nebius \$1.38), not the highest-intensity miners (Applied Digital \$1.43 at $\lambda \approx 0.13$, Core Scientific \$1.44 at $\lambda \approx 0.10$), whose *secured* recovery ($R = 0.55$) more than offsets their intensity. The framework prices the recovery–intensity net, so reading λ off the spread while ignoring seniority would misrank the cohort.

Table 6. Per-issuer credit-adjusted forward $F^{g}(t_0, T_3)$ in \$/hr, holding the commodity branch at $G^{g} = \$1.49$, RFV face $V = \$2.58$, and $L^{\text{op}} = \$0.04$ (all issuer-agnostic) and varying only intensity λ^{term} and seniority-implied recovery $R^{(\text{bk})}$: $S = e^{-2\lambda^{\text{term}}}$, $L^{\text{rec}} = R^{(\text{bk})} V (1-S)$, $F^{g} = S\,G^{g} + L^{\text{rec}} - L^{\text{op}}$. The λ^{term} are representative midpoints of Table 5; the spot–credit correction Γ is negligible outside the distressed regime. Secured high-intensity issuers (Applied Digital, Core Scientific) price near the hyperscaler and project-finance names — recovery offsets intensity — above the unsecured neoclouds.

Issuer	Class	λ^{term}	$R^{(\text{bk})}$	S	L^{rec}	F^{g}
AWS / GCP / Azure	Hyperscaler parent	0.01	0.35	0.98	0.02	1.44
Hut 8 (River Bend)	Project-finance (IG)	0.003	0.55	0.99	0.01	1.45
CoreWeave	Neocloud (unsec.)	0.07	0.35	0.87	0.12	1.37
Nebius	Neocloud (unsec.)	0.06	0.35	0.89	0.10	1.38
Core Scientific	Miner-pivot (sec.)	0.10	0.55	0.82	0.26	1.44
Applied Digital	Miner-pivot (sec.)	0.13	0.55	0.77	0.33	1.43

© 2026 by the author(s). Distributed under a Creative Commons CC BY license.

Preprints.org (www.preprints.org) | NOT PEER-REVIEWED | Posted: 23 June 2026 doi:10.20944/preprints202606.1651.v1

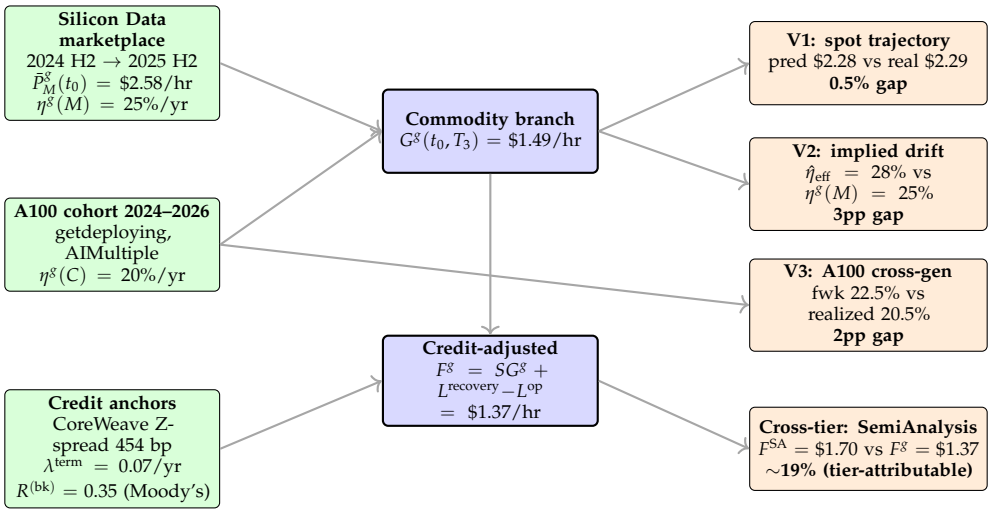

Figure 2. Data flow for the H100 worked example. Green: empirical sources with framework-symbol mappings; blue: framework outputs; orange: validations with realized-vs-predicted gaps. Within-tier and cross-generation validations (V1, V2, V3) achieve gaps of 0.5–3%; cross-tier vs SemiAnalysis exhibits the expected tier-attributable gap.

In-scope universe and validations.

We fix the priced universe *ex ante*: transferable marketplace/cohort-median tiers (Silicon Data marketplace, DePIN, exchange-listed reservations) on NVIDIA GPUs spanning at most one generational transition, with hyperscaler on-demand (administered) and cross-tier comparisons out of scope, so the in-scope claims stand on their own. Figure 2 reports the realized-vs-predicted gaps. The two in-sample checks hold: the within-state path $\$2.58\,e^{-0.25t}$ tracks the marketplace decline to 0.5% and 3% at 6 and 12 months (V1), and the endpoint-implied drift $\hat{\eta}_{\text{eff}} = -\ln(\$1.95/\$2.58) \approx 28\%/\text{yr}$ runs ~3pp hot of the roadmap-set 25% anchor (V2), a genuine realized-vs-anchor comparison rather than a tautology, since the anchor is not endpoint-fit. The clean out-of-sample test is cross-generational (V3): the H100-calibrated framework applied to A100 from Q1 2023 (anchor ~$3.00/hr, Paperspace [62], 3-yr tenor) predicts ~22.5%/yr and $F \approx \$1.53/\text{hr}$ against a realized $1.62/hr (AIMultiple [63]; 20.5%/yr), within 2pp without re-calibration. Out of scope, A100 on-demand declines ~9pp slower (administered-tier inertia, V4, getdeploying [64]), and a two-generation V100 reach is directional only (V5, Amazon Web Services [65]). Table 7 consolidates the tests by evidentiary class.

Baselines: does the lifecycle machinery earn its complexity?

On the out-of-sample A100 test (V3), against the realized Q1 2026 cohort median $1.62/hr the lifecycle forward ($1.53, −5.6%) beats three naive predictors on the same anchor:

$$\text{random walk } \$3.00\,(+85\%), \quad \text{flat carry } \$3.38\,(+109\%), \quad \text{constant-decay } \$3.00\,e^{-0.25\cdot 3}{=}\$1.42\,(-12.5\%).$$

These are deliberately naive baselines — a no-depreciation null, the textbook cost-of-carry forward, and the single-rate practitioner default (the price-side analogue of hyperscalers' straight-line GPU depreciation, here at the realized ~25%/yr) — not the market benchmarks we turn to next. It roughly halves the error of the best foil (constant-decay) and dominates the level-based predictors by shifting drift across the $M \to C$ transition the tenor spans; inside a single state it collapses to constant-decay, so the apparatus earns its complexity only on transition-spanning forwards.

Benchmarks: market forward curves and compute futures.

A genuine external benchmark for (24) now exists: vendor GPU forward curves to 36 months (Silicon Data [66]) and the cleared, cash-settled compute futures already noted (CME Group and Silicon Data [6]; Intercontinental Exchange [7]). These price the forward directly but reduced-form — a no-arbitrage term structure or a cleared quote on a spot index — a number, not a decomposition: no

© 2026 by the author(s). Distributed under a Creative Commons CC BY license.

Preprints.org (www.preprints.org) | NOT PEER-REVIEWED | Posted: 23 June 2026 doi:10.20944/preprints202606.1651.v1

Table 7. Validation scorecard for the worked example. The three prediction tests (in-sample V1, over-identifying V2, out-of-sample V3) probe the commodity branch, which carries the bulk of the price; V3 — the H100-calibrated model applied to A100 without recalibration — is the clean out-of-sample check. The ablation confirms the lifecycle machinery beats the best naïve foil; the tier-basis row is a *consistency* check (it attributes a gap to tier-mix, not a prediction); recovery and the cross-tier hedge are low-power by construction (two realized defaults; an N=18-month panel). The sharpest external check still to come — G^g against the cleared CME/ICE futures strip, a credit-free index (CME Group and Silicon Data [6]; Intercontinental Exchange [7]) — arrives as those contracts settle.

Quantity	Model	Benchmark / data	Result	Class
Spot path, H100	$\$2.58\, e^{-0.25t}$	Silicon Data marketplace	0.5–3% @ 6/12 mo	in-sample (V1)
Drift, H100	25% anchor	endpoint-implied 28%	3 pp	over-identifying (V2)
Forward, A100	\$1.53 (22.5%)	realized \$1.62 (20.5%)	5.6% / 2 pp	**out-of-sample (V3)**
vs. naïve foils	\$1.53 (5.6%)	constant-decay \$1.42 (12.5%)	halves error	ablation
Tier basis	\$1.37 marketplace	SemiAnalysis \$1.70	∼19% attributable	consistency
Recovery $R^{(\mathrm{bk})}$	0.35	2022 cohort 0.15–1.00	inside range	low power (n=2)
Cross-tier hedge $\beta_{\phi\|P}$	−0.3	tier series (N=18)	marginal sig.	exploratory

split of commodity from credit, no obsolescence transition, no issuer-specific default. The framework here is complementary and structural, supplying exactly those channels. Comparison must match the object: the index futures are credit-diversified, so they benchmark the *commodity* branch G^g, whereas the single-issuer credit branch is validated separately by the per-issuer sample (Table 5); a tier-matched test of G^g against the on-demand forward curve is the sharpest external check, available as these series mature.

Cross-tier comparison: SemiAnalysis forward index.

The SemiAnalysis H100 one-year forward index (SemiAnalysis [67]) recorded \$1.70/hr in October 2025, a ∼19% gap above the framework's marketplace-tier \$1.37/hr. Its index sits closer to Silicon Data's neocloud tier (\$2.99–\$3.50/hr), consistent with tier-mix rather than framework error.

Föllmer–Schweizer cross-tier hedge ratio.

Let $\phi(t) = P^{\text{neo-tier}}(t)/P^{\text{mkt-tier}}(t)$, so $F^{\mathrm{SA}}(t,T) \approx \phi(t)\cdot F^g(t,T)$. The Föllmer–Schweizer covariation under $\tilde{\mathbb{Q}}$ gives

$$\xi_t^{FS,\mathrm{SA}} \;=\; \phi(t)\cdot\xi_t^{FS} \;+\; F^g(t,T)\cdot\beta_{\phi|P}(t), \quad \beta_{\phi|P} = \frac{d\langle\phi, P^{\text{mkt-tier}}\rangle}{d\langle P^{\text{mkt-tier}}\rangle}. \tag{25}$$

The Silicon Data tier series (Silicon Data [41]; $N = 18$ months) puts $\phi(t) \in [1.13, 1.36]$ and gives $\hat{\beta}_{\phi|P} \approx -0.3 \pm 0.15/\$$ (95% CI $[-0.6, 0]$), so $\xi^{FS,\mathrm{SA}} \approx 0.60 + \$1.37\,(-0.3) \approx 0.19$, some 68% below the naive $\phi\,\xi^{FS} = 0.60$. With significance marginal at $N = 18$ (Newey–West widening the band to the opposite-sign region), we treat the basis-covariation channel as *exploratory* and prefer within-tier hedging (V1–V2), with a wide buffer (±6% or larger) where cross-tier exposure is unavoidable.

Sensitivity to lifecycle and recovery parameters.

Table 8 reports one-at-a-time perturbation sensitivity of $F^g(t_0, T_3)$ to the four anchor parameters $(\bar{T}, \sigma, m_C/m_M, R^{(\mathrm{bk})})$ around base case.

© 2026 by the author(s). Distributed under a Creative Commons CC BY license.

Preprints.org (www.preprints.org) | NOT PEER-REVIEWED | Posted: 23 June 2026 doi:10.20944/preprints202606.1651.v1

Table 8. One-at-a-time perturbation sensitivity of $F^g(t_0, T_3)$ around base case ($\bar{T} = 30$mo, $\sigma = 6$mo, $m_C/m_M = 0.6$, $R^{(\mathrm{bk})} = 0.35$); $\lambda^{(\mathrm{term})} = 0.07/\mathrm{yr}$. Realized-compute $R^{(\mathrm{bk})}$ range spans the 2022 cohort (Compute North $R \approx 0.15$; Core Scientific $R \approx 1.00$ via reorganization continuation; Compute North Holdings, Inc. [47]; Core Scientific, Inc. [48]).

Parameter	Low	Base	High	F^g low / high ($/hr)	Range vs base
$\bar{T}_{M\to C}$ (months)	24	30	36	\$1.21 / \$1.43	−12% / +4%
$\sigma_{M\to C}$ (months)	3	6	12	\$1.43 / \$1.30	+4% / −5%
m_C/m_M	0.5	0.6	0.7	\$1.34 / \$1.39	−2% / +1%
$R^{(\mathrm{bk})}$ (Moody's bracket)	0.25	0.35	0.50	\$1.34 / \$1.42	−2% / +4%
$R^{(\mathrm{bk})}$ (realized compute)	0.15	0.35	1.00	\$1.31 / \$1.59	−5% / +16%

The transition anchor $\bar{T}$ dominates: a 24-month early transition compresses F^g by ∼12%. σ is moderate (±4–5%) and m_C/m_M small (±1–2%); recovery is ±2–4% in the Moody's bracket and $-5\%/+16\%$ across the realized compute-issuer range. Because $R^{(\mathrm{bk})}$ is high-impact and thinly observed (the realized range rests on two 2022 data points), we treat it not as a constant but as a random recovery with the 2022-cohort spread (mean ≈ 0.35, support $[0.15, 1.00]$), quoting F^g with the resulting $-5\%/+16\%$ band. Transition-timing and recovery are the priority calibration targets; the rest are sub-dominant relative to the ±5% credit-cohort dispersion and ∼19% cross-tier basis.

8. Conclusions

The paper applies established credit-intensity and Föllmer–Schweizer hedging methodology to compute capacity contracts via two domain-specific structural choices. The shared discrete-state lifecycle Markov chain $\zeta(g, t)$ couples commodity drift and bankruptcy intensity; for a single issuer the obsolescence loading on the intensity is pinned by the issuer's own credit spread and scales along the roadmap through the depth ratio of (11), with its cross-issuer heterogeneity deferred to the multi-issuer setting. The Föllmer–Schweizer cross-tier hedge ratio $\xi_t^{FS,\mathrm{SA}} = \phi \cdot \xi_t^{FS} + F^g \cdot \beta_{\phi|P}$ decomposes the cross-tier exposure into multiplicative-ratio and basis-covariation channels by the chain rule for product semimartingales; an exploratory regression on a short monthly panel ($N = 18$, marginal significance) suggests the basis-covariation magnitude lies below the multiplicative shortcut, short of a calibrated hedge ratio. Tractability is established by closed-form affine survival, the H100 example (within-tier gaps 0.5% and 3%), a naive benchmark on which the lifecycle-state model halves the best one-parameter foil's error, the Applied Digital calibration, and an A100 cross-generation out-of-sample test within 2pp (plus a directional V100 reach). The framework prices forward-curve shape, not absolute spot level.

Use as a pricing reference.

The cleared venues price the commodity, credit-free; the bilateral contracts that transact carry a named issuer's default and the hardware's obsolescence, which no traded instrument spans. The framework supplies that single-name layer — the compute analogue of valuing a corporate bond off the curve plus an issuer spread. It can anchor fair value in a bilateral negotiation, supply a counterparty credit-valuation adjustment on a book of compute exposures (wrong-way Γ included), mark balance-sheet and GPU-collateralized-loan positions to model, and frame a hedge against the index (the Föllmer–Schweizer ratio, with the unspanned credit residual flagged). It is a fair-value reference rather than a quote: the commodity leg is validated out-of-sample while the issuer overlay is calibrated to traded spreads, so an output is a band, not a point, and tightens as single-name forwards and the new compute futures (CME Group and Silicon Data [6]; Intercontinental Exchange [7]) mature.

© 2026 by the author(s). Distributed under a Creative Commons CC BY license.

Preprints.org (www.preprints.org) | NOT PEER-REVIEWED | Posted: 23 June 2026 doi:10.20944/preprints202606.1651.v1

References

1. xAI. New Compute Partnership with Anthropic. xAI press release, 2026. Accessed June 2026.
2. Core Scientific, Inc.. Core Scientific and CoreWeave Announce $1.2 Billion Expansion at Denton, TX Site. Core Scientific Investor Relations press release, 2025. Accessed June 2026.
3. Hut 8 Corp.. Hut 8 Signs 15-Year, 245 MW AI Data Center Lease at River Bend Campus with Total Contract Value of $7.0 Billion. Hut 8 press release via PR Newswire, 2025. Accessed June 2026.
4. Applied Digital Corporation. Applied Digital Announces New U.S.-Based High Investment-Grade Hyperscaler Tenant at Delta Forge 1, a 430 MW AI Factory Campus. Applied Digital Investor Relations press release, 2026. Accessed June 2026.
5. S&P Global Market Intelligence. Bitcoin Miners Pivot to AI and HPC as Cryptocurrency Market Slumps. S&P Global Market Intelligence research note, 2026. Accessed June 2026.
6. CME Group.; Silicon Data. CME Group and Silicon Data Partner to Launch First Compute Futures. CME Group press release, 2026. SDH100RT cash-settled GPU compute futures. Accessed June 2026.
7. Intercontinental Exchange. ICE and Ornn to Launch GPU Compute Futures Contracts. ICE Investor Relations press release, 2026. OCPI cleared-futures complex (H100, H200, B200, RTX 5090). Accessed June 2026.
8. Architect Financial Technologies. Architect Financial Technologies Partners with Compute Index Provider Ornn to Launch Exchange-Traded Futures on GPU and RAM Prices. PR Newswire press release, 2026. AX Exchange perpetual futures on the Ornn Computing Power Price Index. Accessed June 2026.
9. Compute Exchange. NVIDIA H100 GPU Price in 2026: New, Refurbished, and Used. Compute Exchange research note, 2026. Accessed June 2026.
10. Amazon Web Services. Amazon EC2 Capacity Blocks for ML can be shared across multiple accounts. AWS What's New announcement, 2026. Accessed June 2026.
11. Föllmer, H.; Sondermann, D. Hedging of non-redundant contingent claims. In *Contributions to Mathematical Economics*; Hildenbrand, W.; Mas-Colell, A., Eds.; North-Holland, 1986; pp. 205–223.
12. Föllmer, H.; Schweizer, M. Hedging of contingent claims under incomplete information. In *Applied Stochastic Analysis*; Davis, M.H.A.; Elliott, R.J., Eds.; Gordon and Breach, 1991; pp. 389–414.
13. Biagini, F.; Cretarola, A. Local risk-minimization for defaultable claims with recovery process. *Applied Mathematics & Optimization* **2012**, *65*, 293–314.
14. Bielecki, T.R.; Jeanblanc, M.; Rutkowski, M. Hedging of defaultable claims. In *Paris-Princeton Lectures on Mathematical Finance 2003*; Springer, 2004; Vol. 1847, *Lecture Notes in Mathematics*, pp. 1–132.
15. Lando, D. On Cox processes and credit risky securities. *Review of Derivatives Research* **1998**, *2*, 99–120.
16. Duffie, D.; Pan, J.; Singleton, K.J. Transform analysis and asset pricing for affine jump-diffusions. *Econometrica* **2000**, *68*, 1343–1376.
17. Hull, J.; White, A. CVA and wrong-way risk. *Financial Analysts Journal* **2012**, *68*, 58–69.
18. Capponi, A.; Figueroa-López, J.E.; Nisen, J. Pricing and semimartingale representations of vulnerable contingent claims in regime-switching markets. *Mathematical Finance* **2014**, *24*, 250–288.
19. Frye, J. Collateral damage. *Risk* **2000**, *13*, 91–94.
20. Brigo, D.; Chourdakis, K.; Bakkar, I. Counterparty risk valuation for energy-commodities swaps: impact of volatilities and correlation. *Energy Risk* **2009**.
21. Cao, Z.; Huang, S. Pricing Portfolios of Compute Capacity Contracts: Cross-Issuer Dependence and Segment Classification. Working paper.
22. Xing, Y. AI Token Futures Market: Commoditization of Compute and Derivatives Contract Design. *arXiv preprint arXiv:2603.21690* **2026**.
23. Tvedt, J. Valuation of VLCCs under income uncertainty. *Maritime Policy & Management* **1997**, *24*, 159–174.
24. Koekebakker, S.; Adland, R.; Sødal, S. Pricing freight rate options. *Transportation Research Part E: Logistics and Transportation Review* **2007**, *43*, 535–548.
25. Duffie, D.; Singleton, K.J. Modeling term structures of defaultable bonds. *The Review of Financial Studies* **1999**, *12*, 687–720.
26. Bielecki, T.R.; Rutkowski, M. *Credit Risk: Modeling, Valuation and Hedging*; Springer Finance, Springer, 2002.
27. Ballotta, L.; Fusai, G.; Marazzina, D. Integrated structural approach to credit value adjustment. *European Journal of Operational Research* **2019**, *272*, 1143–1157.
28. Ghamami, S.; Goldberg, L.R. Stochastic intensity models of wrong way risk: wrong way CVA need not exceed independent CVA. *Journal of Derivatives* **2014**, *21*, 24–46.

© 2026 by the author(s). Distributed under a Creative Commons CC BY license.

Preprints.org (www.preprints.org) | NOT PEER-REVIEWED | Posted: 23 June 2026 doi:10.20944/preprints202606.1651.v1

29. Brigo, D.; Morini, M.; Pallavicini, A. *Counterparty Credit Risk, Collateral and Funding: With Pricing Cases for All Asset Classes*; Wiley, 2013.
30. Gregory, J. *The xVA Challenge: Counterparty Credit Risk, Funding, Collateral, and Capital*, 3rd ed.; Wiley, 2015.
31. Battiston, S.; Mandel, A.; Monasterolo, I.; Roncoroni, A. Climate Credit Risk and Corporate Valuation. CEPR Discussion Paper 20239, Centre for Economic Policy Research, 2025.
32. Kaldor, N. Speculation and Economic Stability. *The Review of Economic Studies* **1939**, *7*, 1–27.
33. Brennan, M.J. The Supply of Storage. *American Economic Review* **1958**, *48*, 50–72.
34. Gibson, R.; Schwartz, E.S. Stochastic convenience yield and the pricing of oil contingent claims. *The Journal of Finance* **1990**, *45*, 959–976.
35. Lucia, J.J.; Schwartz, E.S. Electricity Prices and Power Derivatives: Evidence from the Nordic Power Exchange. *Review of Derivatives Research* **2002**, *5*, 5–50.
36. Cartea, Á.; Figueroa, M.G. Pricing in electricity markets: A mean reverting jump diffusion model with seasonality. *Applied Mathematical Finance* **2005**, *12*, 313–335.
37. Davis, M.H.A. Pricing weather derivatives by marginal value. *Quantitative Finance* **2001**, *1*, 305–308.
38. Bessembinder, H.; Lemmon, M.L. Equilibrium pricing and optimal hedging in electricity forward markets. *The Journal of Finance* **2002**, *57*, 1347–1382.
39. Routledge, B.R.; Seppi, D.J.; Spatt, C.S. Equilibrium forward curves for commodities. *The Journal of Finance* **2000**, *55*, 1297–1338.
40. Ma, S. Technological Obsolescence. NBER Working Paper 29504, National Bureau of Economic Research, 2021.
41. Silicon Data. H100 Rental Price Over Time (2023–2025): A Complete Market Analysis. Silicon Data market analysis, 2025. Tier-stratified median price series (hyperscaler / marketplace / neocloud) across 2023 H2–2025 H2. Accessed June 2026.
42. IntuitionLabs. H100 Rental Prices Compared: $1.49–$6.98/hr Across 15+ Cloud Providers. IntuitionLabs cross-provider GPU pricing analysis (includes V100 and A100 cross-generation context), 2025. Accessed June 2026.
43. CNBC. The Question Everyone in AI Is Asking: How Long Before a GPU Depreciates? CNBC, 2025. Per-generation efficiency roughly doubles to triples on a near-annual cadence; power-dominated TCO renders frontier-class grades uneconomic in 18–36 months; the GPU economic-life debate (Nadella, Burry). Accessed June 2026.
44. Introl. GPU Cloud Prices Collapse: the H100 Rental Market, December 2025. Introl market report, 2025. H100 rental decline driven substantially by oversupply (300+ providers, AWS price cut) and a subsequent supply-tightening rebound, a market transition distinct from obsolescence. Accessed June 2026.
45. WhiteFiber. Understanding the GPU Lifecycle. WhiteFiber technical note, 2025. GPU redeployment across training, inference, and infrastructure tiers; both rental price and utilization decline with grade age. Accessed June 2026.
46. Stanley Laman. Why GPU Useful Life Is the Most Misunderstood Variable in AI Economics. Signals and Noise, 2025. Hardware-collateralized debt is under-collateralized when economic life (∼2–3yr) falls short of underwritten life (∼5–6yr); salvage erosion triggers covenants. Accessed June 2026.
47. Compute North Holdings, Inc.. Voluntary Petition for Relief Under Chapter 11 of the Bankruptcy Code. United States Bankruptcy Court, Southern District of Texas (Houston Division), Case No. 22-90273, filed 22 September 2022, 2022. Accessed June 2026.
48. Core Scientific, Inc.. Voluntary Petition for Relief Under Chapter 11 of the Bankruptcy Code. United States Bankruptcy Court, Southern District of Texas (Houston Division), Case No. 22-90341, filed 21 December 2022, 2022. Emerged January 2024. Accessed June 2026.
49. Duffie, D. Defaultable Term Structure Models with Fractional Recovery of Par. Working paper, Graduate School of Business, Stanford University, 1998.
50. Jarrow, R.A.; Turnbull, S.M. Pricing derivatives on financial securities subject to credit risk. *The Journal of Finance* **1995**, *50*, 53–85.
51. Berd, A.M.; Mashal, R.; Wang, P. Defining, Estimating and Using Credit Term Structures. Working paper; arXiv:0912.4609.
52. Casas Vivas, A. Fractional Recovery of Face Value in Sovereign Bond Markets. SSRN Working Paper 4892668.
53. Cheng, P.; Scaillet, O. Linear-quadratic jump-diffusion modeling. *Mathematical Finance* **2007**, *17*, 575–598.

© 2026 by the author(s). Distributed under a Creative Commons CC BY license.

Preprints.org (www.preprints.org) | NOT PEER-REVIEWED | Posted: 23 June 2026 doi:10.20944/preprints202606.1651.v1

54. Cox, J.C.; Ingersoll, J.E.; Ross, S.A. A theory of the term structure of interest rates. *Econometrica* **1985**, *53*, 385–407.
55. Vasicek, O. An equilibrium characterization of the term structure. *Journal of Financial Economics* **1977**, *5*, 177–188.
56. Duffee, G.R. Term premia and interest rate forecasts in affine models. *The Journal of Finance* **2002**, *57*, 405–443.
57. Fitch Ratings. Fitch Awards First-Time BB- Rating to CoreWeave; Senior Unsecured Notes Rated BB-/RR4. Fitch Ratings press release, May 19, 2025, 2025. Issuer Default Rating BB- with positive outlook; $1.5B senior unsecured notes rated BB-/RR4 (31-50% expected recovery). Accessed June 2026.
58. BondbloX. CoreWeave 9.25% Senior Unsecured Notes due 2030. BondbloX bond market data, 2026. Z-spread 454.1 bp, YTM 8.65% (secondary market). Accessed June 2026.
59. Moody's Investors Service. Annual Default Study. Moody's Default and Recovery Database, 2025. Senior-unsecured 5-year average recovery 35.6 cents/dollar (ending June 2025). Accessed June 2026.
60. Amazon Web Services. Amazon EC2 Service Level Agreement. AWS EC2 SLA, 2026. Tier structure: 10% credit (< 99.99% uptime), 30% credit (< 99%), 100% credit (< 95%). Accessed June 2026.
61. Applied Digital Corporation. Applied Digital Announces Pricing of $2.35 Billion of Senior Secured Notes. Applied Digital Investor Relations press release, 2025. 9.250% senior secured notes due 15 December 2030, issued by APLD ComputeCo LLC at 97% of par; $2.35 billion aggregate principal. Accessed June 2026.
62. Paperspace. GPU Cloud Pricing Comparison. Paperspace cross-provider A100/V100 pricing comparison, 2023. Accessed June 2026.
63. AIMultiple. Cloud GPU Rental Price Index. AIMultiple research aggregator (monthly snapshots, V100/A100/H100 cohort medians, 2024–2026), 2026. Accessed June 2026.
64. getdeploying. NVIDIA A100 Cloud Pricing. getdeploying.com cross-provider GPU pricing aggregator (162 on-demand listings, mid-2026), 2026. Accessed June 2026.
65. Amazon Web Services. New Amazon EC2 Instances with Up to 8 NVIDIA Tesla V100 GPUs (P3). AWS News Blog, 2017. p3.2xlarge (1x V100) on-demand $3.06/hr at launch. Accessed June 2026.
66. Silicon Data. Silicon Data Unveils First GPU Forward Curve. Silicon Data news room, 2026. No-arbitrage implied-forward on-demand rental term structure to 36 months; normalized for spec, interconnect, and region. Accessed June 2026.
67. SemiAnalysis. H100 GPU 1-Year Rental Price Index. SemiAnalysis pricing dataset, 2025–2026. Accessed June 2026.

Disclaimer/Publisher's Note: The statements, opinions and data contained in all publications are solely those of the individual author(s) and contributor(s) and not of MDPI and/or the editor(s). MDPI and/or the editor(s) disclaim responsibility for any injury to people or property resulting from any ideas, methods, instructions or products referred to in the content.

© 2026 by the author(s). Distributed under a Creative Commons CC BY license.